

<sup>1</sup> Key Laboratory of Environmental Change and Natural Disaster, College of Resources Science and Technology, Beijing Normal University, Beijing, China

<sup>2</sup> Bjerknes Center for Climate Research/Nansen Environmental and Remote Sensing Center, University of Bergen, Norway

<sup>3</sup> Nansen-Zhu International Research Center, IAP, Beijing, China

## Reconstruction of Northern Hemisphere 500 hPa geopotential heights back to the late 19th century

D.-Y. Gong<sup>1,2</sup>, H. Drange<sup>2,3</sup>, and Y.-Q. Gao<sup>2,3</sup>

With 13 Figures

Received December 12, 2005; revised March 31, 2006; accepted July 27, 2006

Published online • •, 2006 © Springer-Verlag 2006

### 18 Summary

19 In this study the authors have developed a statistical method  
20 and have reconstructed Northern Hemisphere 500 hPa  
21 heights back to the late 19th century using one temper-  
22 ature and three sea level pressure (SLP) data sets. First, the  
23 relationship between ERA40 500 hPa heights and surface  
24 temperature and SLP was screened using stepwise multiple  
25 regression based on the calibration period of 1958–2002  
26 (1998/2000 according to the availability of SLP data).  
27 All selected predictors (temperature and SLP) were signif-  
28 icant and their variance contribution was greater than 1%.  
29 On average, there were 8.1 variables retained in the final  
30 regression equations. Second, the regression equations  
31 were applied to compute the 500 hPa height through to  
32 the late 19th century for the whole Northern Hemisphere.  
33 As the SLP and temperature coverage improved over  
34 time, the number of predictors decreased by about 1 in the  
35 most recent periods, and the root mean squared error de-  
36 creased by about 0.8 m. A leave-one-out cross-validation  
37 method was used to test the skill and stability of the  
38 regression models. The reduction of error during the cross-  
39 validation period of 1958–1997 varied from 0.33 to 0.56,  
40 depending on the SLP data. Reconstructions were also  
41 checked using NCEP/NCAR 500 hPa heights from  
42 January 1949 to December 1957, and compared with the  
43 historical reconstruction over Europe. Reconstructions  
44 show high consistency with these independent data sets.  
45 Generally, the reconstruction provides a valuable oppor-  
46 tunity to analyze, as well as to validate climate simulations

of the variability in free atmosphere circulations over the 47  
past one hundred years. 48  
49

### 1. Introduction 50

The analysis of historical atmospheric tropospheric 51  
circulation is critically important to global and 52  
regional climate change and extremes with regard 53  
to its dynamical features (e.g. Luterbacher 54  
et al., 2000; Casty et al., 2005a). Long-term ob- 55  
servations of sea level pressure (SLP) across the 56  
Northern Hemisphere have been available since 57  
the late 19th century. Investigations of climate 58  
indices derived from SLP (such as the Arctic 59  
Oscillation/North Atlantic Oscillation, Southern 60  
Oscillation, and so on) has greatly enriched our 61  
knowledge of how and why large-scale climate 62  
has varied over the last one hundred years or so. 63  
In addition to the historical climate analysis, there 64  
is increasing interest in the assessment of his- 65  
torical atmospheric circulation variability as sim- 66  
ulated by climate models (Casty et al., 2005b; 67  
Raible et al., 2005). However, global/hemispheric 68  
analyses of the free atmosphere are confined to 69  
much shorter periods of about 50 years because 70

1 routine observations of global upper-level circula-  
 2 tion have been available only since the early  
 3 1950s. The short length of upper level data ham-  
 4 pers our better understanding of global climate  
 5 change. It is important and necessary to recon-  
 6 struct historical geopotential height fields and to  
 7 extend as far back as possible for both climate  
 8 study and climate simulation validation. There are  
 9 several approaches for computing or estimating  
 10 500 hPa heights.

- 11 (i) The direct method is to add the 500–  
 12 1000 hPa thickness to the 1000 hPa height.  
 13 This method is based on physical relation-  
 14 ships, since the thickness is proportional to  
 15 the mean temperature of the air column be-  
 16 neath the 500 hPa level (e.g. Polansky, 2002).  
 17 This approach requires local SLP and tem-  
 18 perature data, which are often missing in the  
 19 early period and which should be interpo-  
 20 lated or reconstructed in advance, which in  
 21 itself introduces additional uncertainties or  
 22 biases.
- 23 (ii) The second approach is to use climate mod-  
 24 els to simulate the atmospheric circulation  
 25 forced by observed boundary conditions  
 26 such as the sea surface temperature (SST).  
 27 Similarly, missing upper level data may also  
 28 be filled by reanalysis using only surface  
 29 data (Compo et al., 2006). These methods es-  
 30 sentially take into account the atmospheric  
 31 internal dynamics. For example, Bengtsson  
 32 et al. (2004) assessed the long term trends  
 33 in reanalysis data sets based on model out-  
 34 put under fixed observation distribution and  
 35 quality. A successful simulation relies heav-  
 36 ily on the well-documented surface data.  
 37 Unfortunately, the quality and/or availability  
 38 of the historical surface boundary data, in-  
 39 cluding SST, snow cover, sea ice and so on,  
 40 are generally low in the 19th century and  
 41 early 20th century (Houghton et al., 2001,  
 42 Chapter 2). Furthermore, the results of sim-  
 43 ulation vary with the skill or performance  
 44 of climate models (Houghton et al., 2001,  
 45 Chapter 8), and the ratios of signal/noise in  
 46 geopotential heights are often higher in the  
 47 tropics than the high latitudes in SST-forced  
 48 simulations.
- 49 (iii) The most frequently used approach is to com-  
 50 pute upper level heights using the statistical

51 regression method. Regional to large-scale  
 52 surface climate is strongly related to the near  
 53 surface and upper level atmospheric circula-  
 54 tion (Klein and Yang, 1986; Houghton et al.,  
 55 2001). The relationship is consistent irre-  
 56 spective of upscaling (the local scale is re-  
 57 lated to large scale) or downscaling (the large  
 58 scale is related to the local scale), the links  
 59 can be determined and often quantitatively  
 60 presented as specification relationship in  
 61 weather and climate analysis. Therefore, geo-  
 62 potential heights can be derived from surface  
 63 data using the reverse specification method.  
 64 In early works this idea was adopted to fill  
 65 in missing observations in some areas or  
 66 stations (e.g. Namias, 1944). Klein and Dai  
 67 (1998) developed the idea and computed  
 68 monthly mean 700 hPa heights with a reso-  
 69 lution of  $10^\circ \times 10^\circ$  for 1947–1992 over  
 70 the western half of the Northern Hemi-  
 71 sphere from station temperature, precipita-  
 72 tion, and SLP. The merit of this method is  
 73 that it takes into account the relationship  
 74 between surface climate and upper-air cir-  
 75 culation. Therefore, it is often used to  
 76 compute heights and atmospheric circula-  
 77 tion indices. For example, Gong and Wang  
 78 (2000) examined the possibility of comput-  
 79 ing Northern Hemisphere 500 hPa heights  
 80 from 1873 using Jones’ SLP (Jones, 1987)  
 81 and surface temperature data. Luterbacher  
 82 et al. (2002) reconstructed SLP and 500 hPa  
 83 heights across Europe back to AD1500 using  
 84 principal components analysis (PCA) regres-  
 85 sion. Schmutz et al. (2001) used the same  
 86 predictors as Klein and Dai (1998), i.e., SLP,  
 87 temperature, and precipitation to reconstruct  
 88 the monthly 700, 500, and 300 hPa heights  
 89 in the European and Eastern North Atlantic  
 90 regions for the period 1901–1947. They ap-  
 91 plied canonical correlation analysis based  
 92 on PCA filtered predictors. Using this kind  
 93 of statistical approach, Brönnimann and  
 94 Luterbacher (2004) filled the gaps in upper  
 95 level circulation data during the period of  
 96 World War II over the Northern Hemisphere.  
 97 The importance of other predictors such as  
 98 radiosonde data, wind direction and cloud ob-  
 99 servation as well as ship logbook informa-  
 100 tion related to wind for the pre-1850 period  
 101 has been recently highlighted (García-Herrera

et al., 2005). For example, Brönnimann et al. (2004) and Brönnimann and Luterbacher (2004), show that upper level radiosonde data (e.g. Brönnimann, 2003) can be used as an important predictor when computing atmospheric circulation over large areas. However, these upper level observations exist for short time periods only and are sparse in space. Therefore, in our study we employed only surface temperature and SLP records.

The purpose of this paper is to objectively reconstruct 500 hPa heights for the entire Northern Hemisphere back to 1871 by using the reverse specification approach. Data and the method of stepwise regression are summarized in Sect. 2. The properties of the regression equations are presented in Sect. 3. Our reconstructions are compared with other different data sets, and the reconstructive error/skill is estimated in Sect. 4. The usefulness of the reconstruction is discussed in Sect. 5. Finally, Sect. 6 presents the brief conclusion.

## 2. Data and method

### 2.1 Data preparation

There are several long-term surface temperature and SLP data sets available since the mid-late 19th century. These are used as predictor data for the reconstruction period. Here we considered three SLP and one temperature data sets, all

of them are of hemispheric or global coverage (Table 1) and are summarized below.

- (i) HadSLP1, also known as GMSLP3. This is an updated version from GMSLP21f which consists of in-situ marine and land station monthly SLP observations, and is blended with several gridded analysis data sets (from Australia and the USA) to create globally complete fields. The updated version, GMSLP3, is an historical,  $5^\circ \times 5^\circ$  gridded monthly data set covering the period 1871–1998 (Basnett and Parker, 1997).
- (ii) Jones’s SLP for the Northern Hemisphere since 1873 (hereafter referred to as CRUSLP). It is archived on a  $5^\circ$  latitude  $\times$   $10^\circ$  longitude mesh, and is available northward of  $15^\circ$  N (Jones, 1987).
- (iii) National Center for Atmospheric Research (NCAR) SLP, starts in January 1899 and is gridded on a  $5^\circ$  latitude  $\times$   $10^\circ$  longitude mesh (Trenberth and Paolino, 1980).
- (iv) Surface temperature data (HadCRUT2, hereafter denoted as T2 for simplicity) have been obtained from the Climatic Research Unit, University of East Anglia. This data set consists of global land and marine surface temperature anomalies since 1850 (Jones et al., 1999, 2001; Jones and Moberg, 2003; Rayner et al., 2003).

There are some additional gridded SLP data sets available. For example, Kaplan et al. (2000) released a reduced space optimal interpolation SLP (OISLP) with a resolution of  $4^\circ$  latitude  $\times$   $4^\circ$

**Table 1.** Data used for geopotential height reconstruction

Data	Resolution	Coverage	Source
a. SLP data			
HadSLP1	monthly, $5^\circ$ lat. $\times$ $5^\circ$ lon.	Jan. 1871–Dec. 1998, global	Basnett and Parker (1997)
CRUSLP	monthly, $5^\circ$ lat. $\times$ $10^\circ$ lon.	Jan. 1873–Dec. 2000, north of $15^\circ$ N	Jones (1987)
NCARSLP	monthly, $5^\circ$ lat. $\times$ $10^\circ$ lon.	1899–2003, north of $15^\circ$ N	Trenberth and Paolino (1980)
b. Surface temperature			
HadCRUT2	monthly, $5^\circ$ lat. $\times$ $5^\circ$ lon.	Jan. 1870–Dec. 2003, global	Jones and Moberg (2003), Rayner et al. (2003)
c. 500 hPa height			
ERA-40	monthly, $2.5^\circ$ lat. $\times$ $2.5^\circ$ lon.	Jan. 1958–Dec. 2001, global	<a href="http://data.ecmwf.int/data/d/era40_daily">http://data.ecmwf.int/data/d/era40_daily</a>

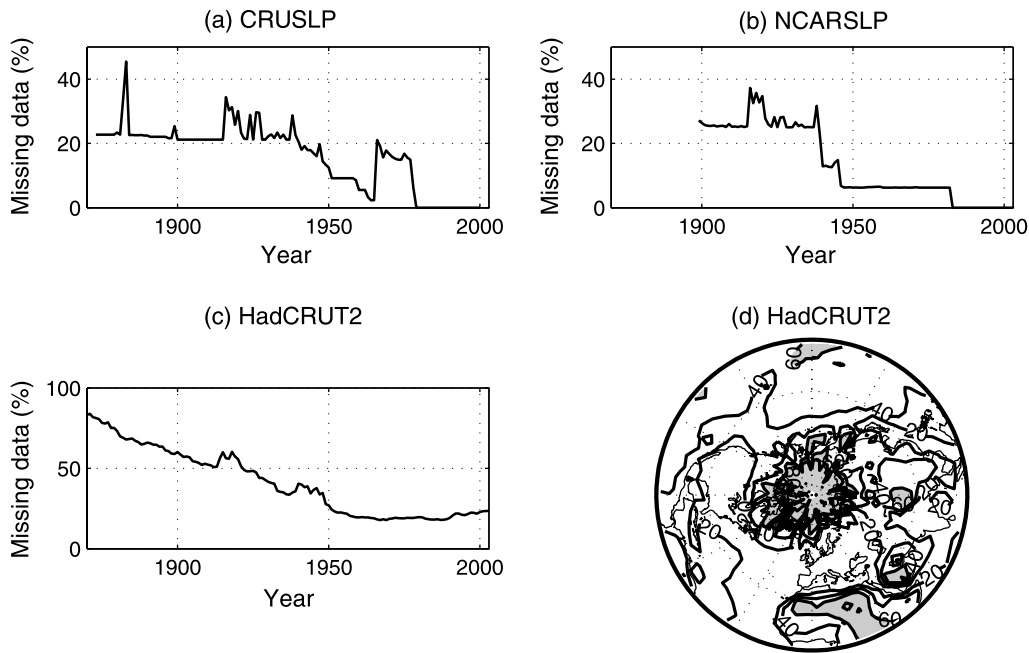


**Fig. 1.** Missing data (in percentage) for SLP and temperature fields. (a) CRUSLP, north of  $15^{\circ}$  N; (b) NCARSLP, north of  $15^{\circ}$  N; (c) HadCRUT2 temperature, north of  $0^{\circ}$  N; (d) the distribution of missing data in HadCRUT2 is for period 1856–2003, areas in excess of 60% are shaded

1 longitude over global seas for April 1854–  
 2 December 1992, which is computed using the  
 3 leading 80 empirical orthogonal functions, based  
 4 on the Comprehensive Ocean–Atmosphere Data  
 5 Set (COADS) data sets. Since this data set covers  
 6 only oceans, it has not been used in the present  
 7 study. In addition, it should be noted that SLP  
 8 over oceans in HadSLP1 heavily relies on the  
 9 quality and availability of COADS SLP records.  
 10 In the present study HadSLP1 pressure data have  
 11 been used, therefore the exclusion of OISLP  
 12 would not reduce the potential SLP information  
 13 over oceans.

14 For CRUSLP, NCARSLP, and T2, coverage  
 15 before the 1950s is low, but improved gradually  
 16 since this time (Fig. 1). Figure 1d shows the spa-  
 17 tial distribution of missing data in T2. In the  
 18 Arctic Ocean and neighbouring regions, central  
 19 Pacific, and northern Africa the missing data ex-  
 20 ceeds 60%. For the CRUSLP and NCARSLP  
 21 data sets, similar conditions exist. Generally, data  
 22 availability in northern polar regions is poor dur-  
 23 ing the reconstruction period. Among all data  
 24 sets only HadSLP1 is complete. The gaps in the  
 25 original observation are statistically interpolated  
 26 in advance. However, our reconstructions reveal  
 27 that the interpolation provides no additional in-  
 28 formation which would result in a better recon-

struction. Similar features were also found in the  
 HadSLP2 data (Allan and Ansell, 2006).

The predictand data used here are ECMWF  
 (European Centre for Medium-Range Weather  
 Forecast) 40-year reanalysis (ERA40) 500 hPa  
 heights available from September 1957–August  
 2002 which are archived on a regular  $2.5^{\circ} \times 2.5^{\circ}$   
 grid. After re-sampling we used a  $5^{\circ} \times 5^{\circ}$  resolu-  
 tion sub-data set in our reconstruction. It should  
 be pointed out that differences exist between in-  
 strumental station data and gridded data, arising  
 from many sources such as the original data un-  
 certainty, quality control procedure, interpolation  
 method, and so on. Reanalysis 500 hPa is different  
 from the observations. These differences might  
 be profound, despite reanalysis relying heavily  
 on observations.

## 2.2 Methodology

Of the statistic approaches available, some tech-  
 niques are more widely used than others. One is  
 the climate field reconstruction (CFR) technique  
 (e.g. Smith et al., 1996; Jones and Mann, 2004;  
 Brönnimann and Luterbacher, 2004; Rutherford  
 et al., 2003, 2005; Mann et al., 2005; Casty et al.,  
 2005a; Xoplaki et al., 2005, among others), which  
 does not assume any a priori local relationship

29  
30  
31  
32  
33  
34  
35  
36  
37  
38  
39  
40  
41  
42  
43  
44  
45  
46  
47  
48  
49  
50  
51  
52  
53  
54

1 between predictors and the climatic field being  
 2 reconstructed, and depends more heavily on as-  
 3 sumptions about the stationarity of relationships  
 4 between the predictors and large-scale patterns of  
 5 climate variability than the local calibration tech-  
 6 nique (Jones and Mann, 2004; Rutherford et al.,  
 7 2005, and references therein for further infor-  
 8 mation). As a result, the CFR approach often  
 9 produces a smoother reconstruction. However,  
 10 the quality of the reconstruction may depend not  
 11 only on the number/density and quality of predic-  
 12 tors but also on the specific locations, since this  
 13 determines whether or not key large-scale patterns  
 14 of variance are likely to be captured. In parti-  
 15 cular, large-scale climate patterns derived from  
 16 fewer predictors easily drift or can be distorted.  
 17 Recently, some authors performed the so-called  
 18 independent climate field reconstruction using  
 19 a number of different parameters. Interestingly  
 20 each reconstruction shared no common predictor  
 21 (Casty et al., 2005a, c). This enables the relation  
 22 of the fields to one another and helps investigate  
 23 the possible dynamics and interactions between  
 24 climate variables.

25 Alternatively, local multivariate regression is  
 26 a ‘classic’ technique (e.g. Klein and Dai, 1998;  
 27 Gong and Wang, 2000, among many others),  
 28 which allows one to screen all possible local pre-  
 29 dictors, even those which are remotely located.  
 30 Possible teleconnections may be identified and  
 31 included, helping to increase the reconstruction  
 32 skill. This is particularly true when there are  
 33 spare observations. Since our aim is to recon-  
 34 struct the historical 500 hPa heights as skillfully  
 35 as possible, we did not test the independent re-  
 36 construction. To make use of as much predictive  
 37 information as possible, we prefer to employ the  
 38 local regression technique, using combined pre-  
 39 dictors (SLP plus surface temperature). Inter-  
 40 estingly, in dense data areas such as Europe, the  
 41 local regression and PCA-based reconstructions  
 42 produce highly similar results (see Sect. 4.3).

43 In the present study we employ a stepwise  
 44 regression technique to reconstruct the histor-  
 45 ical 500 hPa heights. The regression equations  
 46 between surface climate variables (temperature  
 47 and SLP) and the predictand (ERA40 500 hPa  
 48 heights) are derived for the calibration period  
 49 from 1958. The relationship is then applied to  
 50 the early time period from the late 19th century to  
 51 1957, to compute the 500 hPa heights. According

to the available predictor data sets, three recon- 52  
 struction experiments were carried out, namely 53  
 (a) HadSLP1 + T2 experiment, (b) CRUSLP + T2 54  
 experiment, and (c) NCARSLP + T2 experiment. 55  
 The procedure is summarized below: 56

- (i) All data, including the predictor and predict- 58  
 and data sets, were adjusted and presented 59  
 as anomalies with respect to 1961–1990. 60  
 All missing data were simply removed. To 61  
 maintain a consistent spatial resolution with 62  
 surface temperature and SLP, the 500 hPa 63  
 height predictand data were prepared on a 64  
 $5^\circ \times 5^\circ$  mesh. The reconstructed 500 hPa 65  
 heights cover 1368 grids (19 in latitude and 66  
 72 in longitude) extending from  $90^\circ$  N,  $0^\circ$  E, 67  
 to  $0^\circ$  N,  $355^\circ$  E.
- (ii) After the predictand ERA40 500 hPa height 69  
 at a specific grid-point and month was se- 70  
 lected, the predictor data matrix, which con- 71  
 sists of six variables including temperature 72  
 and SLP for the concurrent month (denoted 73  
 as month 0), as well as for two adjacent 74  
 months, i.e. the previous one month (denoted 75  
 as month  $-1$ ) and the later one month 76  
 (denoted as month  $+1$ ), over the whole 77  
 Northern Hemisphere, for each of the three 78  
 reconstruction experiments was prepared. 79  
 The Calibration period for case HadSLP1 + 80  
 T2 is 1958–1998, for case CRUSLP + T2 81  
 is 1958–2000, and for case NCARSLP + T2 82  
 T2 is 1958–2001. Surface climate is often 83  
 related to upper level atmospheric circula- 84  
 tion with a time lag. Thus, the use of 85  
 surface temperature and SLP in month 86  
 ( $-1$ ) and month ( $+1$ ) as predictor candi- 87  
 dates can provide additional information, 88  
 particularly in the early period when the 89  
 observations are sparse. This selection of 90  
 months has also been used by Klein and 91  
 Dai (1998), Gong and Wang (2000) and 92  
 Brönnimann and Luterbacher (2004).
- (iii) It should be pointed out that compared to the 93  
 sample size the number of candidate vari- 94  
 ables is very large. Prior to the analysis the 95  
 candidates were screened by simply com- 96  
 puting correlations ( $R$ ) between predictors 97  
 and ERA40 500 hPa heights, and those vari- 98  
 ables with moderate-high correlations were 99  
 screened out. Many of the  $|R|$  values were 100  
 rather small, representing low or no skill in 101

1 predicting height. These low skill variables  
 2 were excluded from the stepwise regression  
 3 process. However, the large data matrix,  
 4 would require large computing resources, or  
 5 could even result in computing error and  
 6 instability during matrix manipulation. A  
 7 better way to avoid this is to remove these  
 8 low-skill variables prior to the regression.  
 9 This low skill threshold was determined at  
 10  $|R| > 0.25$  (approximately the 90% confi-  
 11 dence level). The screening was carried out  
 12 locally, grid-point by grid-point and month  
 13 by month, using the entire calibration period  
 14 data. The result being the inclusion of the  
 15 most predictive predictors in a much smaller  
 16 predictor matrix. This screening process re-  
 17 duced the predictor matrix about 40%. Most  
 18 importantly, this screening process does not  
 19 reduce the reliability of the finally results.  
 20 In most of cases the number of variables in  
 21 the final regression equation remained the  
 22 same when  $|R|$  increased from 0 to 0.1, and  
 23 changes slightly when  $|R|$  increased from  
 24 0.1 to 0.2.

25 (iv) Then stepwise regression was applied to de-  
 26 rive the regression equations between the  
 27 predictand (ERA40 500 hPa heights) and  
 28 temperatures and SLPs. In an ordinary step-  
 29 wise regression approach, the selection and  
 30 removal of variables from the candidate pre-  
 31 dictors are determined according to their sta-  
 32 tistical significance. Here the confidence level  
 33 was set at to 95%, i.e., during the variable-  
 34 selection process any variables entering the  
 35 regression equation must be significant at the  
 36 95% level, and during the variable-removal  
 37 process all predictors not significant at the  
 38 95% level were eliminated. Even following  
 39 the application of pre-process screening, as  
 40 described in step (iii), the predictor matrix  
 41 was still rather large. Theoretically, adding  
 42 more variables to the regression equation  
 43 would increase the explained variance (i.e.  
 44 larger  $R^2$ ) – enough variables are present  
 45 when  $R^2$  approaches 1. In practice, even  
 46 a random time series would input a little  
 47 variance into the equation. However, this  
 48 is meaningless and causes the problem of  
 49 overfitting (Wilks, 1995). Obviously, a vari-  
 50 able contributing only a very small portion  
 51 of the total variance would bring large

uncertainty and bias in the final regression  
 results, even if this variable is statistically  
 significant. In order to produce a stable and  
 robust regression equation, a third criterion  
 was employed: all included variables had to  
 contribute more than 1% of the total var-  
 iance. This rule applies to each single grid-  
 point. Since the available predictors change  
 with time, the number of final predictors may  
 also change with time and grid-point.

(v) Finally, regression equations were employed  
 to compute the 500 hPa height anomalies in  
 the early periods (January 1871–December  
 1957 for HadSLP1 + T2, January 1873–  
 December 1957 for CRUSLP + T2, and  
 January 1899–December 1957 for  
 NCARSLP + T2 case).

### 3. Properties of the final regression equations 69

#### 3.1 Predictor variables 70

Figure 2 shows the number of predictors in the  
 final regression equations. Although the spatial  
 coverage and availability of data is different  
 among these SLP data sets, the number of pre-  
 dictors in the final regression equations was very  
 similar. On average, there were 8.2 predictors for  
 HadSLP1 + T2 and CRUSLP + T2, and 8.1 for  
 NCARSLP + T2, almost the same. The number  
 of predictors varied greatly from grid-point to  
 grid-point and from month to month. The mini-  
 mum number of predictors varied between 1 and  
 3, notice that these minimum numbers appear as  
 the extreme conditions for a couple of grid-points  
 at a specific month and specific year, not an aver-  
 age for the whole Northern Hemisphere over the  
 entire reconstruction period. Among the three  
 cases, the maximum number varied between 15  
 and 20. On average, temperature and SLP ac-  
 counted for 59.3 and 40.7% of the total number  
 of predictors. For a target month, temperature pre-  
 dictors in the current month account for 26.5%,  
 the temperature of month (−1) and month (+1)  
 account for 16.1 and 16.7%, respectively. The  
 SLP in the current month accounts for about  
 24.5%, while the SLP in the adjacent months ac-  
 counts for much lower percentages in all three re-  
 construction experiments (see Fig. 2). Obviously,  
 to predict 500 hPa for the target month, simul-  
 taneous SLP is very important, while temperature

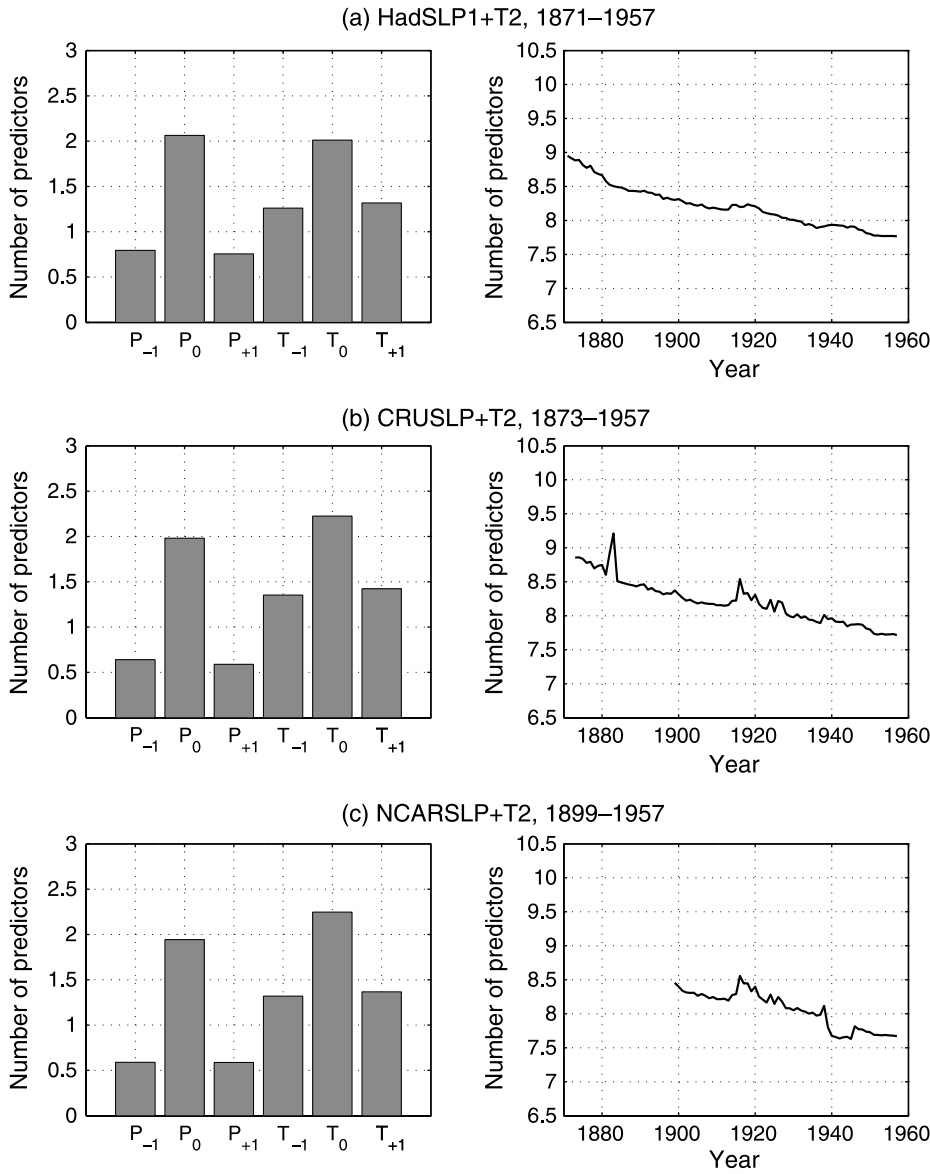


**Fig. 2.** Number of predictors in the final regression equations for the three reconstruction experiments. Shown in the right panel are the changes of the number of variables for each experiment. The mean total number of predictors for whole reconstruction period is shown in the left panels, where ‘P’ and ‘T’ denote SLP and temperature, respectively. The subscripts of ‘0’, ‘-1’, ‘+1’ denote the concurrent, previous one, and next one month, correspondingly

1 predictors in the simultaneous month, as well as in  
 2 the preceding and following months are also very  
 3 important. This may be due to the fact that at-  
 4 mospheric circulation has a short memory in re-  
 5 lation to surface climate anomalies. Temperature  
 6 often has greater persistence. Thus, temperature  
 7 data in the adjacent months can provide a very  
 8 useful indication of the upper level atmospheric  
 9 circulation, either as a preceding surface bound-  
 10 ary forcing for the circulation or as a delayed re-  
 11 sponse to the circulation anomalies in the physical  
 12 sense. Both can establish strong associations be-  
 13 tween 500 hPa heights and surface temperature.  
 14 Therefore, inclusion of SLP and temperature in  
 15 the adjacent months increases the number of  
 16 efficient candidates.

Figure 3 shows the annual cycle of the number of predictors. All three reconstructions show similar features. The number of variables increased

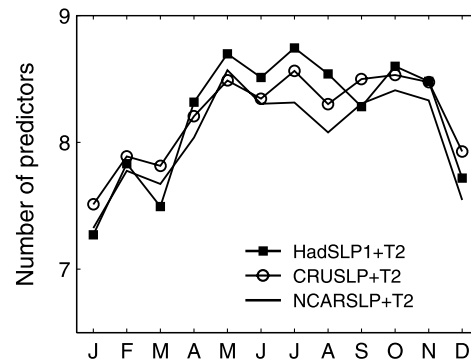


**Fig. 3.** Number of predictors for different months

1 from about 7.4 in January to about 8.5 in July,  
 2 and then dropped to about 7.8 in December. The  
 3 seasonal difference is clearly evident. On average  
 4 the number of predictors in winter (December–  
 5 February) is 7.6. For June–August, the variable  
 6 number is 8.4. This feature is different from Klein  
 7 and Dai (1998) results. In their reconstruction  
 8 of 700 hPa height they used fewer variables in  
 9 May–August than in December–April (see their  
 10 Fig. 3b). Our results suggest that to successfully  
 11 calculate the 500 hPa heights in warm seasons  
 12 more predictors are needed, while the predictor  
 13 number is somewhat lower in cold months. This  
 14 might be due to the fact that in wintertime there  
 15 are active extra-tropical atmospheric modes, as  
 16 well as strong associations between the low-  
 17 frequency variability in surface climate and tropo-  
 18 spheric circulation. In winter, a few independent  
 19 predictors can capture more information on cli-  
 20 mate dynamics.

21 Very often the regression algorithm tends to  
 22 overfit the data by including many variables in the  
 23 equation. In our stepwise regression and screen-  
 24 ing, we employed strict criteria to ensure that only  
 25 the most skillful predictors were selected for the  
 26 final equation. Highly inter-correlated variables  
 27 were optimized where replication of their signifi-  
 28 cant co-variance has been eliminated. The number  
 29 of predictors in the final equation was about 8.  
 30 It is interesting to note that this number is close  
 31 to the results of Klein and Dai (1998), in their  
 32 reconstruction of 700 hPa heights for the Western  
 33 Hemisphere. They found that a multiple regres-  
 34 sion equation with 2–6 independent variables  
 35 usually satisfies the criteria for statistical stability  
 36 and synoptic reasoning. The methods used here  
 37 should be helpful in improving the problem of  
 38 overfitting, but perhaps not the elimination of  
 39 the issue.

### 40 3.2 Goodness of fit

41 Two criteria were used to examine the goodness  
 42 of fit and the performance of the multiple regres-  
 43 sion equations. One is the adjusted square of the  
 44 multiple correlation coefficient (i.e. the adjusted  
 45  $R$  square,  $R_a^2$ ), which is a measure of the actual fit  
 46 of the best-fitting straight line and is equivalent  
 47 to the percent reduction of the unexplained vari-  
 48 ance or reduction of variance. The other is the  
 49 root mean squared error (RMSE), a measure of

absolute error. At any grid-point in any month  
 the RMSE is defined as:

$$\text{RMSE} = \sqrt{\frac{1}{n} \sum_{i=1}^n (\phi - \hat{\phi})^2}$$

where  $\phi$  is the predictand,  $\hat{\phi}$  is the predicted  
 height, and  $n$  is the number of training data.  
 For each year for a specific month, all grid-points  
 were averaged over the Northern Hemisphere to  
 generate an annual value. The average, maximum,  
 and minimum were determined for the entire re-  
 construction period. The statistics of  $R_a^2$  are plot-  
 ted in Fig. 4 to show the possible annual cycle.  
 The features of the three reconstructions differ  
 noticeably from each other. The annual mean  $R_a^2$   
 drops in March for the HadSLP1 + T2 reconstruc-  
 tion, while the conditions for CRUSLP + T2 and  
 NCARSLP + T2 are more stable, with their annu-  
 al mean  $R_a^2$  showing only very slight change with  
 season. The changes in maximum and minimum  
 $R_a^2$  are generally in parallel with annual mean  
 values. For the NCARSLP + T2 case, however,  
 the minimum values in September and October  
 show much a larger departure from the annual  
 mean  $R_a^2$  curve. This is probably caused by the poor  
 data quality in some years (e.g. 1941). Overall,  
 using the criterion of  $R_a^2$ , the reconstruction of  
 CRUSLP + T2 showed the best performance and  
 stability in all three reconstruction cases.

Table 2 presents the annual mean and season-  
 al mean RMSE. In all three reconstructions the  
 RMSE in winter is somewhat larger than in  
 summer. In winter the RMSE is about 10–11 m.  
 While in summer it is between 6 and 7 m, about  
 30–40% smaller. However, this does not neces-  
 sarily mean that the variance explained by the  
 regression equations in winter is much smaller  
 than in summer because the winter variance of  
 500 hPa heights is greater than summer, a con-  
 clusion also confirmed by RMSE which reflects  
 the absolute error rather than the relative error.  
 The annual cycle of RMSE is very similar for  
 all three reconstruction cases, in terms of their  
 seasonal fluctuations as well as their magnitudes.  
 On average, the RMSEs for HadSLP + T2,  
 CRUSLP + T2, and NCARSLP + T2 are 8.57,  
 8.75, and 8.73 m, respectively. The geographical  
 distribution of the RMSE was then checked  
 (Fig. 5). Large errors are located in two centres:  
 one in the Arctic Ocean, and the other in the



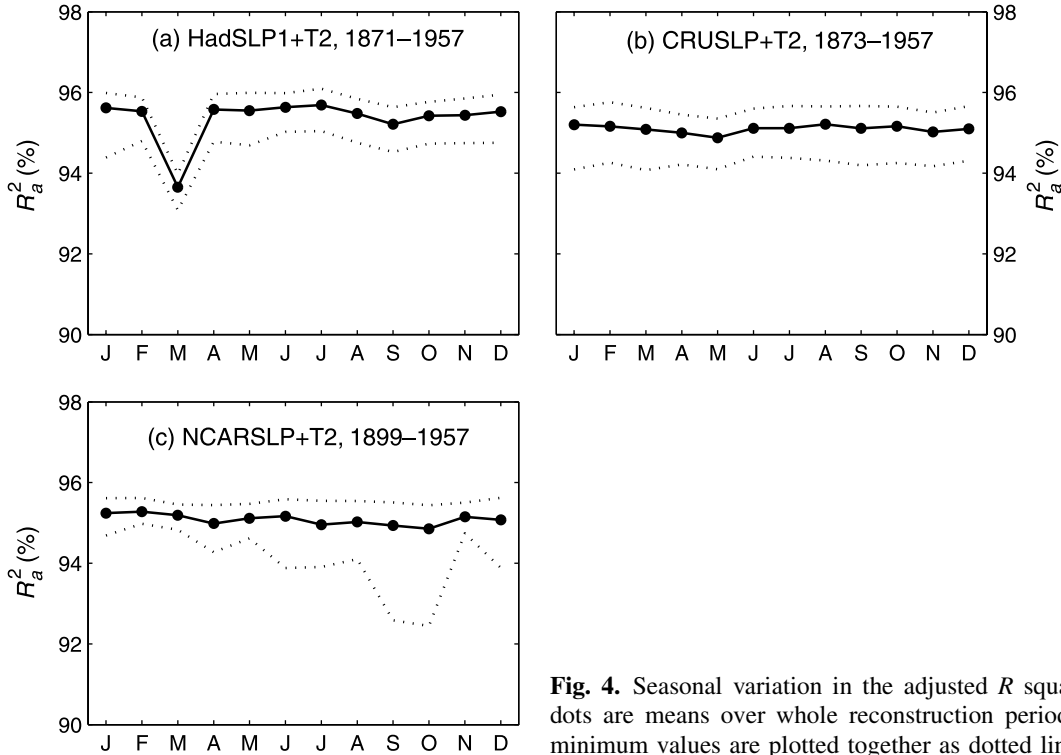


**Fig. 4.** Seasonal variation in the adjusted  $R$  square. Lines with filled dots are means over whole reconstruction period, the maximum and minimum values are plotted together as dotted lines

**Table 2.** Statistics for the root mean squared error of the regression equations. Unit m

	HadSLP1 + T2	CRUSLP + T2	NCARSLP + T2
Dec., Jan., Feb.	10.70	11.0	10.93
Mar., Apr., May	9.16	9.05	8.91
Jun., Jul., Aug.	6.41	6.73	6.84
Sep., Oct., Nov.	8.02	8.20	8.27
Yearly average	8.57	8.75	8.73

1 north Pacific around the Aleutian Islands. The  
 2 RMSE gradually decreases from about 15 m in  
 3 the high latitudes to less than 6 m in the middle  
 4 and low latitudes. All three cases show similar  
 5 spatial features even though there are differ-  
 6 ences in the availability and coverage of SLP,  
 7 suggesting that the regression equations are gen-  
 8 erally stable among the three experiments with  
 9 respect to the fitting errors.

### 10 3.3 The influence of missing data

11 As shown in Sect. 2, the number of missing data  
 12 varies with time. For instance, SLP for Decem-  
 13 ber 1944 is entirely missing in NCARSLP. There are  
 14 many missing values, especially in the first part  
 15 of the 20th century. In the early period there are  
 16 more than 20–50% missing data in all predictor

data (except HadSLP1), after which time data  
 availability improves gradually (Fig. 1). How  
 does the missing data influence the performance  
 of the regression equations? Temporal changes  
 were examined based on (1) the number of vari-  
 ables, (2) RMSE, and (3) the adjusted  $R$  square.  
 Together with the mean number of predictors in  
 Fig. 2 the changes of the number of predictors  
 as a function of time are shown. Obviously, the  
 number of predictors varies with the improve-  
 ment of data coverage and availability. There is a  
 long-term decreasing trend, while during the two  
 of World Wars the number of predictors clearly  
 increased. Through the reconstruction period, the  
 number of predictors dropped by about 1. It is in-  
 teresting to note that the HadSLP1 + T2 displays  
 very similar features to those of CRUSLP + T2  
 and NCARSLP + T2, although HadSLP1 does not

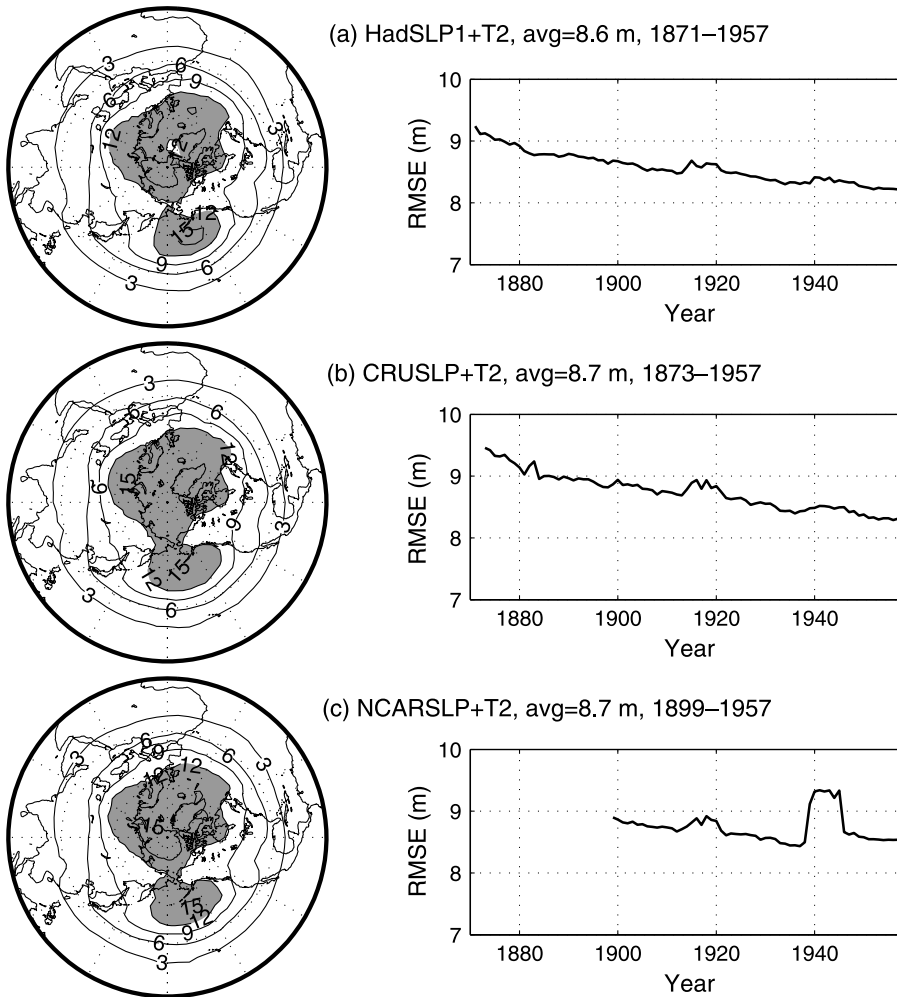


**Fig. 5.** Distribution of the root mean squared errors (RMSE). Regions where values greater than 12 m are shaded in order to highlight the error centers. Their changes with time are shown in the right panel

1 suffer from missing data. This should be due to  
 2 the limitation of availability of the useful infor-  
 3 mation, even though the real missing data in the  
 4 original observations were interpolated by statis-  
 5 tical methods. The meteorological signals con-  
 6 tained in the original observations are essential.  
 7 The interpolation of SLP or temperature cannot  
 8 input additionally useful information for recon-  
 9 struction of the 500 hPa heights.

10 As data availability improved, RMSE decreased  
 11 simultaneously (Fig. 5). In the HadSLP1 + T2 and  
 12 CRUSLP + T2 reconstructions, the errors dropped  
 13 from 9 m in the 1870s to about 8.2 m in the  
 14 1950s. During the two World Wars there are small  
 15 rises. With the exception of NCARSLP + T2,  
 16 which shows a moderate rise during World  
 17 War II. Overall there should be slightly higher  
 18 uncertainty during the early period of reconstruc-  
 19 tions of HadSLP + T2 and CRUSLP + T2. For  
 20 NCARSLP + T2 reconstruction there is somewhat  
 21 larger uncertainty during World War II.

22 Next, temporal changes in the adjusted  $R$   
 23 square were examined. The three cases show sim-  
 24 ilar features: an upward trend through the recon-  
 25 struction period and a notable drop during World  
 26 Wars I and II (figure not shown). From the 1880s  
 27 to the 1950s  $R_a^2$  rose slightly by 1% in both  
 28 HadSLP1 + T2 and CRUSLP + T2 reconstruc-  
 29 tions. In the NCARSLP + T2 experiment the  $R_a^2$   
 30 increased only 0.2% from the 1900s to the 1950s,  
 31 but during World War II it clearly dropped. These  
 32 results indicate that missing data do influence  
 33 the performance of the regression equations.  
 34 The gradual improvement of observation records  
 35 led to a decrease in the number of predictors  
 36 and RMSE, and also resulted in a weak increase  
 37 in  $R_a^2$ , even though long-term changes were small  
 38 in magnitude. With respect to  $R_a^2$  the influ-  
 39 ence of missing data on the stability and perfor-  
 40 mance of the regression equations was somewhat  
 41 smaller for CRUSLP + T2 and HadSLP1 + T2  
 42 reconstructions.

## 1 4. Verification

### 2 4.1 Cross-validation

3 Validation can be used simply to estimate the gen-  
 4 eralization error of a given equation, or it can be  
 5 used for equation selection by choosing one of  
 6 several equations that have the smallest esti-  
 7 mated generalization error. In this case, however,  
 8 there is a short calibration period. If more years  
 9 were retained for validation purposes, the cali-  
 10 bration samples would be smaller and the result  
 11 would very likely produce a regression with higher  
 12 instability and larger error. Instead cross-valida-  
 13 tion was performed by applying a leave-one-out  
 14 method. To facilitate comparison the validation  
 15 period for all three experiments was 1958–1997.  
 16 For each case, each month at each grid-point, cali-  
 17 bration and estimation were repeated 40 times.  
 18 Based on the cross-validation results, the reduc-  
 19 tion of error statistic (RE) (Cook et al., 1994) was  
 20 used as a diagnostic of reconstructive error/skill,  
 21 which is defined as:

$$\text{RE} = 1 - \frac{\sum(\phi - \hat{\phi})^2}{\sum(\phi - \phi_c)^2}$$

23 where  $\phi$  is the ERA40 500 hPa heights,  $\hat{\phi}$  is the  
 24 estimation, and  $\phi_c$  is the mean of the calibration  
 25 period. The computation of RE was carried out  
 26 locally (the sums extend over 40 years, for each  
 27 month) and/or at the hemispheric level (the sums  
 28 extend over both years and grid-points). RE = 0  
 29 represents the threshold for no skill in the recon-  
 30 struction. RE > 0.2 provides an indication of use-  
 31 ful reconstruction.

32 RE scores for all three reconstruction experi-  
 33 ments are summarized in Table 3. CRUSLP + T2  
 34 and NCARSLP + T2 have similar and high  
 35 skills, REs are +0.51 and +0.56, respectively.  
 36 The HadSLP1 + T2 score is somewhat smaller at  
 37 +0.33. The RE scores change with season, maxi-  
 38 mum scores occurring in winter, while lower skills

showing up in summer. This is consistent with 39  
 previous studies (for example Brönnimann and 40  
 Luterbacher, 2004). Interestingly, the seasonal dif- 41  
 ference in CRUSLP + T2 and NCARSLP + T2 42  
 cases is notably smaller than in the HadSLP1 + T2 43  
 experiment. The HadSLP1 + T2 RE in summer 44  
 is 0.18, the smallest in all cases. Moreover, the 45  
 three experiments show differing stability in the 46  
 RE scores from 1958 to 1997. CRUSLP + T2 and 47  
 NCARSLP + T2 have similar, higher stabilities. 48  
 RE scores in the HadSLP1 + T2 models have 49  
 greater year-to-year fluctuations after the late 50  
 1970s (see Fig. 6). These should provide a higher 51  
 level of confidence for the CRUSLP + T2 and 52  
 NCARSLP + T2 reconstructions. 53

The spatial distribution of RE scores are pre- 54  
 sented in Fig. 7. Most of the useful reconstruc- 55  
 tions (RE > 0.2) are located in the extra tropics 56  
 (north of about 30° N). The maximum RE scores 57  
 are located in northern America, northern Pacific, 58  
 northern Atlantic, northwestern Asia, and Europe. 59  
 Compared to other continents, the middle to low 60  
 latitudes of Asia shows relatively small values in 61  
 all three reconstructions. Overall, the RE scores 62  
 are lower in low latitudes in all three experi- 63  
 ments, with minimum centres appearing in north 64  
 Africa and the neighbouring Atlantic, and east 65  
 Pacific about 20–25° N. Additional reconstruc- 66  
 tions were generated using the recently updated 67  
 HadSLP2 data set (Allan and Ansell, 2006). The 68  
 RE scores of which are very similar to HadSLP1 69  
 in terms of temporal features and the spatial 70  
 distribution. 71

To some degree, these features are similar to 72  
 the spatial distribution of the root mean squared 73  
 errors (Fig. 5). RMSE centres are most obvious in 74  
 the Arctic Ocean, where lower RE scores are also 75  
 found (particularly in the HadSLP1 + T2 experi- 76  
 ment). The error centre in the northern Pacific, 77  
 however, disappears in the RE maps. Instead, 78  
 the northern Pacific is characterised by high re- 79  
 constructive skills. Brönnimann and Luterbacher 80

**Table 3.** The RE scores for cross-validation period 1958–1997

	HadSLP1 + T2	CRUSLP + T2	NCARSLP + T2
Dec., Jan., Feb.	0.55	0.60	0.64
Mar., Apr., May	0.31	0.50	0.57
Jun., Jul., Aug.	0.18	0.47	0.58
Sep., Oct., Nov.	0.30	0.47	0.47
Annual	0.33	0.51	0.56

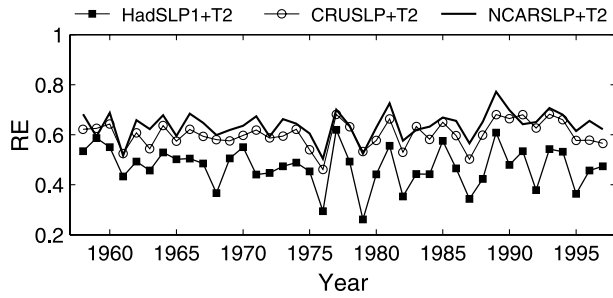


**Fig. 6.** Time series of the RE scores for the cross-validation period of 1958–1997

1 (2004) RE scores for 700 hPa and 500 hPa recon-  
 2 structions for the 1939–1944 period also have  
 3 very similar spatial features (c.f. their Fig. 2).  
 4 Low and high reconstructive skills seem to be  
 5 confined to geographical locations, whether these  
 6 relate to the predictability of atmospheric circula-  
 7 tion or to data availability and quality are ques-  
 8 tions which need further discussion.

#### 9 4.2 Comparison with NCEP/NCAR reanalysis 10 500 hPa heights

11 This subsection further compares the reconstruc-  
 12 tions with National Centers for Environmental  
 13 Prediction/National Center for Atmospheric Re-  
 14 search (NCEP/NCAR) reanalysis data (Kalnay

et al., 1996), which are of the same spatial reso- 15  
 lution of  $2.5^\circ \times 2.5^\circ$  as ERA-40 data but covers a 16  
 longer time period. Thus, 500 hPa heights for a 17  
 pre-calibration period of 1949–1957 were used 18  
 as independent observation data for verification. 19  
 The regression stability and the data quality of 20  
 the computed 500 hPa heights were checked in the 21  
 conventional way. The consistency between the 22  
 reconstruction and NCEP/NCAR reanalysis can 23  
 easily be judged by the spatial correlations of 24  
 the height anomalies. Circulation patterns often 25  
 experience high spatial autocorrelation, reducing 26  
 the efficient number of degrees of freedom. The 27  
 significance level of the spatial correlation can be 28  
 estimated using the Monte Carlo method by ran- 29  
 domly re-arranging the variable order. Since this 30  
 study focussed on generating the reconstructions 31  
 strict significant tests were not conducted. Here 32  
 the correlations were simply computed from all 33  
 1368 grid-points. Data in high and low latitudes 34  
 are dealt equally. Correlations were calculated for 35  
 each month for each of the three reconstruction 36  
 cases. Figure 8 shows the results for all months 37  
 during 1949–1957 (108 months in total). The 38  
 CRUSLP + T2 and NCARSLP + T2 reconstruc- 39  
 tions display smaller month-to-month differ- 40  
 ences, suggesting more stable consistency with 41  
 NCEP/NCAR reanalysis 500 hPa heights. Mean 42

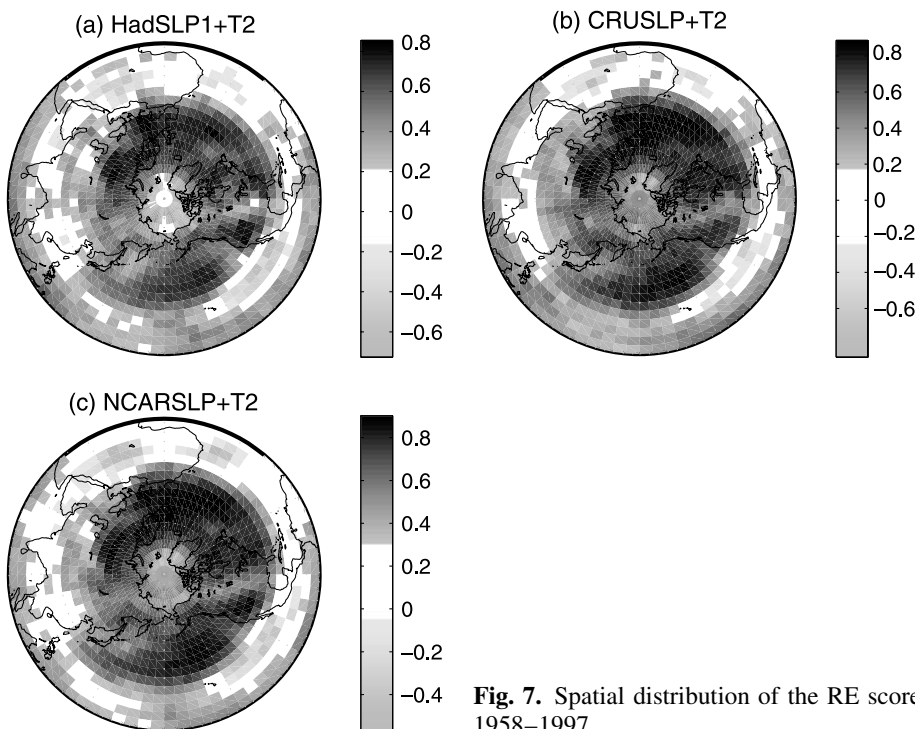


**Fig. 7.** Spatial distribution of the RE scores for the cross-validation period of 1958–1997

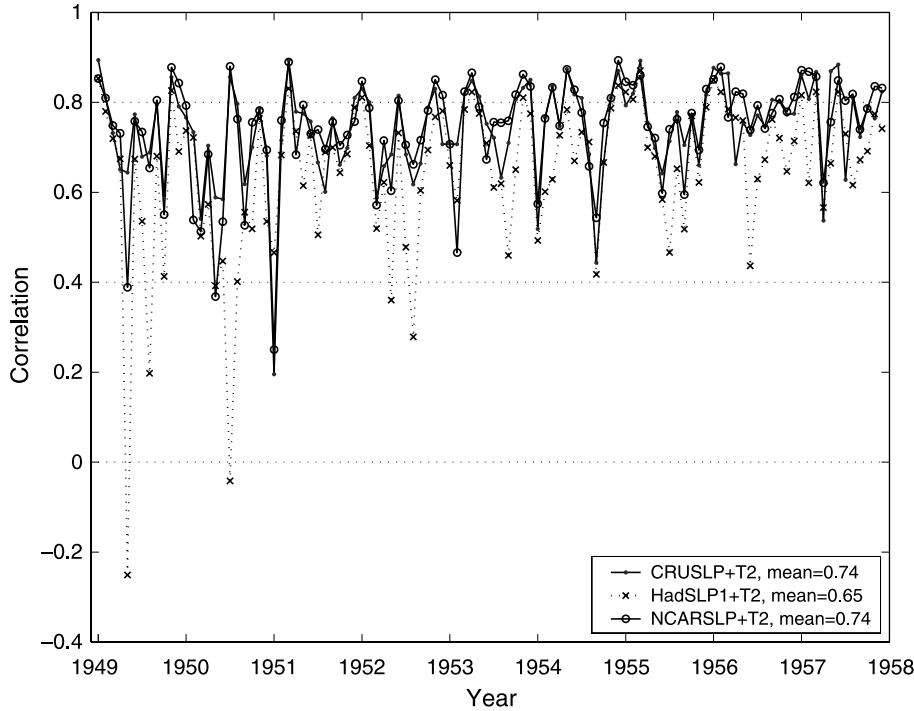


**Fig. 8.** Spatial correlation coefficients between the computed 500 hPa height anomalies and NCEP/NCAR reanalysis height anomalies over northern hemisphere. Three cases are plotted together for comparison

1 spatial correlations are also the same, 0.74. The  
 2 HadSLP1 + T2 reconstruction shows a much larger  
 3 month-to-month difference in the correlation,  
 4 especially in the early 1950s. Two months with low  
 5 correlation are outstanding. One is July 1950,  
 6 with correlation near zero, and the other is May  
 7 1949, with a negative correlation of  $-0.25$ . The  
 8 mean spatial correlation in 1949–1957 is 0.65,  
 9 smaller than the other two reconstructions. The  
 10 reason(s) why HadSLP1 + T2 reconstruction is dif-  
 11 ferent from other two cases are however, as yet,  
 12 unclear.

13 The seasonal cycle of the spatial correlations is  
 14 evident in HadSLP1 + T2, changing from 0.72 in  
 15 winter to only 0.57 in summer. While for the  
 16 CRUSLP + T2 and NCARSLP + T2 reconstruc-  
 17 tions the seasonal difference is almost indistin-

18 guishable, varying slightly between 0.76 and 0.73  
 19 (see Table 4).

20 To demonstrate how consistent the spatial pat-  
 21 terns are between the reconstructions and NCEP/  
 22 NCAR reanalysis 500 hPa height anomalies, the  
 23 similarity in their features has been examined.  
 24 Figure 9 displays an example for January 1957.  
 25 In the NCEP/NCAR reanalysis map, the positive  
 26 anomaly centres are located in the northern Pacific,  
 27 East Asia, southern U.S., and Europe. A negative  
 28 centre appears in eastern Canada and Greenland.  
 29 These features are fairly well reproduced in the  
 30 CRUSLP + T2 reconstruction, their spatial correla-  
 31 tion is 0.86. The other two reconstructions contain  
 32 similar features. For example, the NCARSLP + T2  
 33 is correlated with NCEP/NCAR reanalysis at  
 34 0.87 (Fig. 9).

**Table 4.** Statistics for the spatial correlations between reconstruction and NCEP/NCAR reanalysis 500 hPa height. Based on 9-year period of January 1949–December 1957 (108 months)

	HadSLP1 + T2	CRUSLP + T2	NCARSLP + T2
Dec., Jan., Feb.	0.72	0.76	0.76
Mar., Apr., May	0.65	0.74	0.73
Jun., Jul., Aug.	0.57	0.73	0.74
Sep., Oct., Nov.	0.66	0.73	0.75
Maximum	0.87	0.89	0.89
Minimum	$-0.25$	0.20	0.25
Average	0.65	0.74	0.74

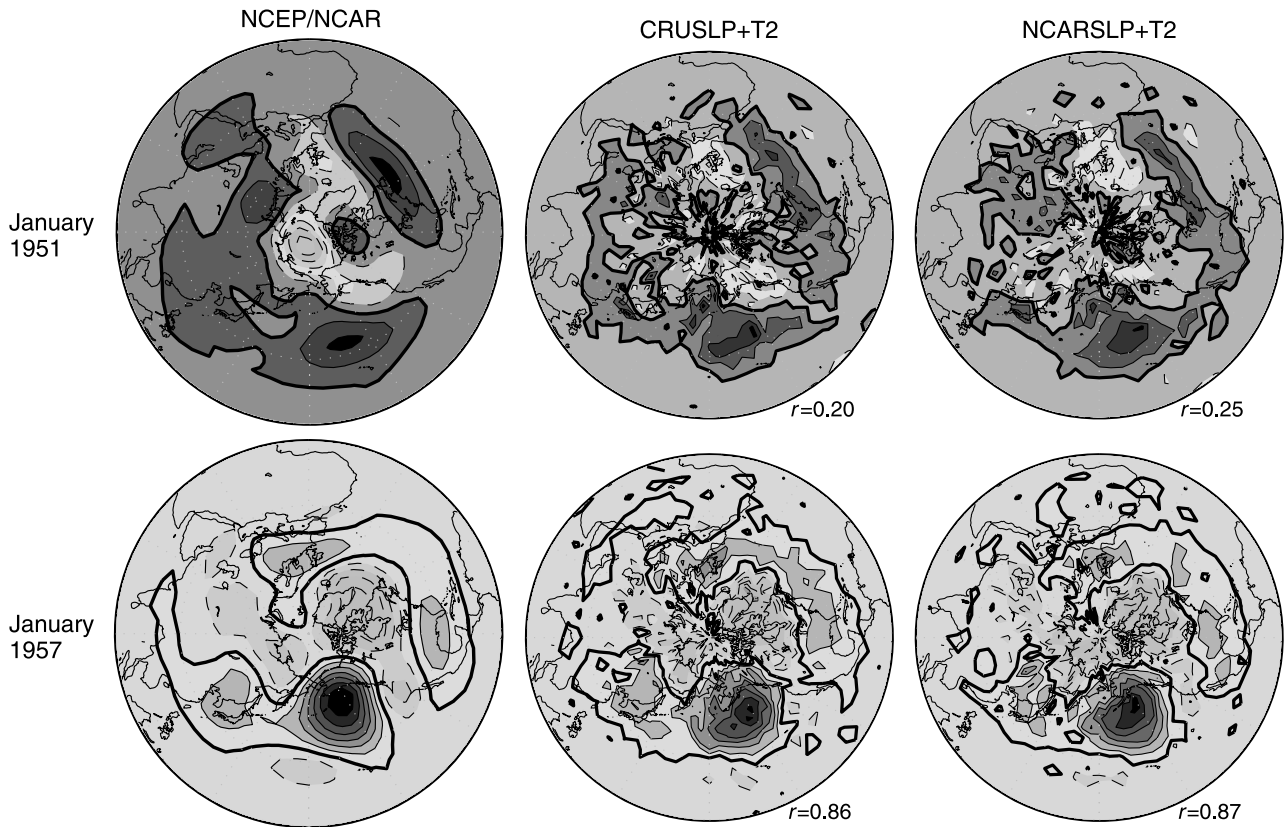


**Fig. 9.** Reconstructed 500 hPa height anomalies from CRUSLP + T2 and NCARSLP + T2 experiments for January 1951 and January 1957. Compared with NCEP/NCAR reanalysis 500 hPa height anomalies. Spatial correlation with NCEP/NCAR are shown too. Zero contours are shown in bold, positive contours are shown in solid lines, and negative contours are in dashed lines. Contour intervals: 40 m

1 Figure 8 shows there are some low correlations for several months. As an example, Fig. 9  
 2 displays the CRUSLP + T2 reconstruction for January 1951. The correlation with NCEP/NCAR  
 3 500 hPa heights is only +0.20, the lowest in all 108 months of CRUSLP + T2 reconstructions.  
 4 It is very interesting to note that even though the overall spatial correlation is low, there is  
 5 good consistency in the mid-low latitudes. In particular the pattern of the anomalous centres  
 6 in the northern Pacific, northern Atlantic and Ural Mountains is very similar. The positions  
 7 and intensities of mid-latitude anomalous centres are also very similar. Unfortunately, a great  
 8 difference shows up over the Arctic regions. The same situation appears in the HadSLP1 + T2 and  
 9 NCARSLP + T2 reconstructions. Figure 9 also shows the NCARSLP + T2 reconstruction for  
 10 January 1951. Although its correlation of 0.25 is the lowest in all NCARSLP + T2 reconstructions,  
 11 the spatial pattern in middle and low latitudes is

22 quite similar to the CRUSLP + T2 reconstruction as well as to the NCEP/NCAR reanalysis. Similar  
 23 conditions exist in other low correlation months. 24

25 The comparison with NCEP/NCAR reanalysis data clearly illustrates that the reconstructions  
 26 in the middle latitudes are of higher consistency among the three reconstruction experiments and  
 27 observations. The discrepancy mainly arises over the Arctic regions. This is likely due to poor data  
 28 availability and probably also due to larger RMSE in northern polar regions. In addition, the dense  
 29 grid in the high latitude contributes a larger portion to the correlation which can distort the correlation  
 30 incorrectly biasing it toward the high latitudes. This can exaggerate the difference between the re-  
 31 construction and NCEP/NCAR reanalysis 500 hPa data and underestimate the spatial correlation. 32  
 33  
 34  
 35  
 36  
 37  
 38

39 The above investigation suggests that the reconstruction reliability in North Pole regions is  
 40 lower than in middle latitudes. In all three reconstructions the CRUSLP + T2 and NCARSLP + T2  
 41  
 42

1 are more consistent with observations during the  
 2 analysis period of 1949–1957.

3 *4.3 Comparison with European reconstruction*

4 Luterbacher et al. (2002) reconstructed gridded sea  
 5 level pressure over the eastern North Atlantic–  
 6 European region (30° W–40° E, 70° N–30° N)  
 7 back to AD1500, using principal component re-  
 8 gression analysis based on a combination of early  
 9 station temperature, pressure, precipitation, and  
 10 documentary proxy data. Using the same proce-

11 dure, they later reconstructed 500 hPa heights on a  
 12  $2.5^\circ \times 2.5^\circ$  grid for the same region using NCEP/  
 13 NCAR reanalysis 500 hPa heights as the predict-  
 14 and based on the calibration period 1948–1990.  
 15 The method and data sets used in their study are  
 16 different from this current study, therefore their  
 17 results are different. In this subsection a compar-  
 18 ison of the current reconstructions with the  
 19 Luterbacher et al. (2002) results are discussed.

20 A grid point for analysis of 0° E, 60° N was  
 21 randomly chosen (Fig. 10). This is an ocean grid-  
 22 point where reconstruction is not usually as good

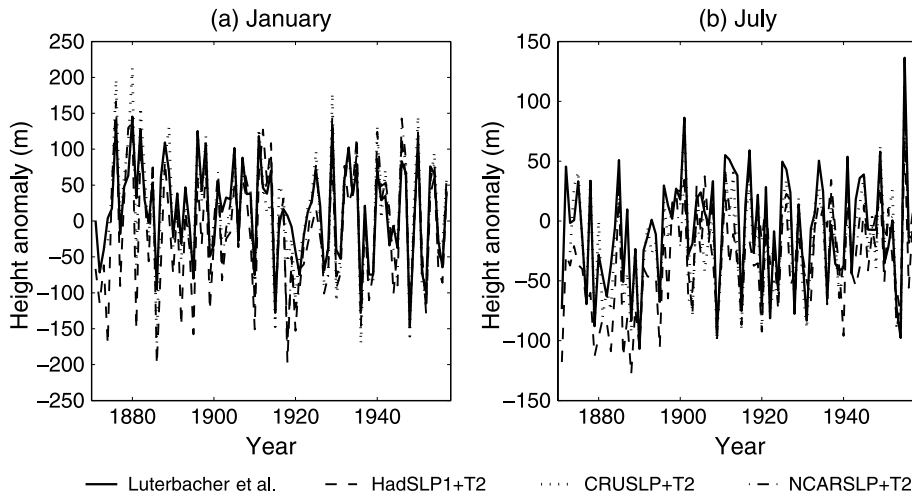


**Fig. 10.** Time series of the reconstructed 500 hPa height anomalies at a grid (0° E, 60° N) for (a) January and (b) July

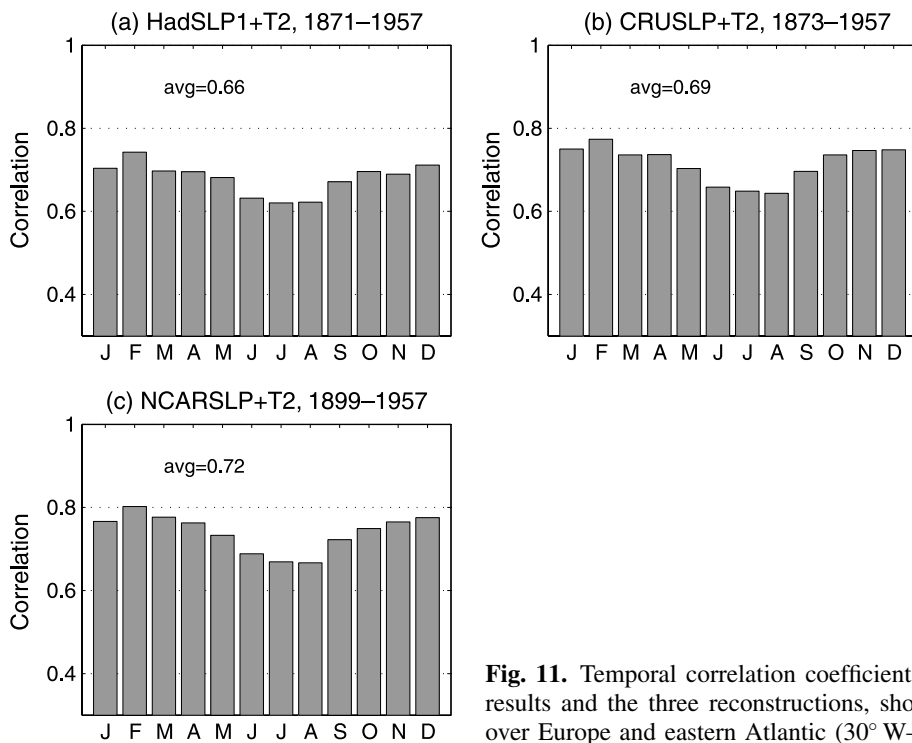


**Fig. 11.** Temporal correlation coefficients between Luterbacher et al. (2002) results and the three reconstructions, shown as the regional means averaged over Europe and eastern Atlantic (30° W–40° E, 70° N–30° N)

1 as for land grid-points. In addition, this grid-  
 2 point does not show the greatest consistency with  
 3 the Luterbacher et al. (2002) results. The three  
 4 reconstructions are plotted together with the  
 5 Luterbacher et al. (2002) values at this grid-point.  
 6 Clearly, all four timeseries vary in-phase with  
 7 very high consistency in both January and July.  
 8 This encourages a comparison for all grid-points.  
 9 Temporal correlations were calculated at each  
 10 grid-point, which were found to be generally high  
 11 in the three reconstructions. The consistency is  
 12 greater over most of Europe, and relatively small  
 13 in some southern grid-points near North Africa  
 14 (figures not shown). To get an idea how the consis-  
 15 tency varies with season, all temporal correlations  
 16 were averaged for each month over the whole  
 17 region. The results are plotted in Fig. 11. Minimum  
 18 correlations occurred in summer (June–August) in  
 19 all three reconstructions, while the maximum cor-  
 20 relations appeared in cold seasons. Annual means  
 21 of the temporal correlations for HadSLP1 + T2,  
 22 CRUSLP + T2, and NCARSLP + T2 are 0.66,  
 23 0.68, and 0.72, respectively. The data sets and  
 24 methods used in our reconstructions are very dif-  
 25 ferent from those of Luterbacher et al. (2002),  
 26 but produced very similar 500 hPa height patterns  
 27 and temporal variability in the eastern North  
 28 Atlantic and European regions. This does not nec-  
 29 essarily mean that the same goodness of fit ap-  
 30 plies equally to other grid-points beyond Europe,  
 31 the consistency between these different recon-  
 32 structions adds additional confidence to the current  
 33 reconstructions with regard to the methodology  
 34 and approach.

## 35 5. Preliminary applications

36 To demonstrate the usefulness of the reconstruc-  
 37 tions, this section briefly shows two preliminary  
 38 applications. One focuses on explaining winter  
 39 temperature extremes in East China, and the other  
 40 tests ENSO related atmospheric anomalies in the  
 41 reconstruction period. In both applications only  
 42 the CRUSLP + T2 reconstruction is employed, be-  
 43 cause it shows better reconstructive skill as dem-  
 44 onstrated in the previous sections.

### 45 5.1 Winter temperature extremes in East Asia

46 Winter temperature extremes in East Asia are of  
 47 importance in monitoring the climate response to

48 global warming. Mid-high latitude Asia has ex-  
 49 perience rapid wintertime temperature varia-  
 50 tions during the last one hundred years or so  
 51 (Houghton et al., 2001). Wang et al. (1999) esti-  
 52 mated the occurrence of very cold winters using  
 53 observation records for Beijing and Shanghai,  
 54 which are the longest observations in China  
 55 available since the late 19th century. Empirical  
 56 orthogonal function analysis of December–  
 57 February mean temperature anomalies showed  
 58 that the leading spatial mode has the same sign  
 59 at almost all stations. This unipole mode ac-  
 60 counts for nearly half of the total variance (49%).  
 61 Therefore, most of the stations experience the  
 62 same or very similar temporal features in winter  
 63 temperature, i.e., the cold temperatures tend to oc-  
 64 cur at many stations simultaneously, mainly due  
 65 to the fact that the East Asian winter monsoon  
 66 dominates over most of east China. Therefore,  
 67 this provides a chance to analyze extremely cold  
 68 winters in the last one hundred years based on a  
 69 couple of stations. Beijing and Shanghai mean  
 70 temperatures provide a reliable alternative esti-  
 71 mation of national average temperatures. Based  
 72 on the long-term observations of temperature  
 73 anomalies ( $T'$ ) for the period 1880–1957 five ex-  
 74 tremely cold winters were identified using the  
 75 criterion of  $T' \leq -1.65\sigma$ , where  $\sigma$  is the standard  
 76 deviation in the whole period 1880–1957. This  
 77 defines a climate extreme at the 95% level for  
 78 a one-tailed  $t$ -test. Extremely cold winters in-  
 79 clude 1884/85 ( $T' = -2.2^\circ\text{C}$ ), 1892/93 ( $-2.7^\circ\text{C}$ ),  
 80 1935/36 ( $-2.8^\circ\text{C}$ ), 1944/45 ( $-2.8^\circ\text{C}$ ), and  
 81 1956/57 ( $-2.2^\circ\text{C}$ ). Similarly, three of the  
 82 warmest winters were identified by the criterion  
 83 of  $T' \geq 1.65\sigma$ , including 1934/35 ( $+1.7^\circ\text{C}$ ),  
 84 1945/46 ( $+1.3^\circ\text{C}$ ), and 1948/49 ( $+1.5^\circ\text{C}$ ).

85 With regard to East Asian temperature varia-  
 86 bility and extremes many recent studies have  
 87 paid more attention to near surface circulation  
 88 systems such as the Siberian High in the SLP  
 89 field (Gong and Wang, 1999; Gong and Ho,  
 90 2002, 2004; Wu and Wang, 2002). To get a better  
 91 understanding of the mid-tropospheric circulation  
 92 anomalies in association with the winter temper-  
 93 ature extremes, a composite analysis based on  
 94 the warmest three and coldest five winters iden-  
 95 tified above was conducted. Figure 12 displays  
 96 the 500 hPa difference (warmest winters minus  
 97 coldest winters). A well-defined features show up:  
 98 strong negative anomalies appear in a broad region



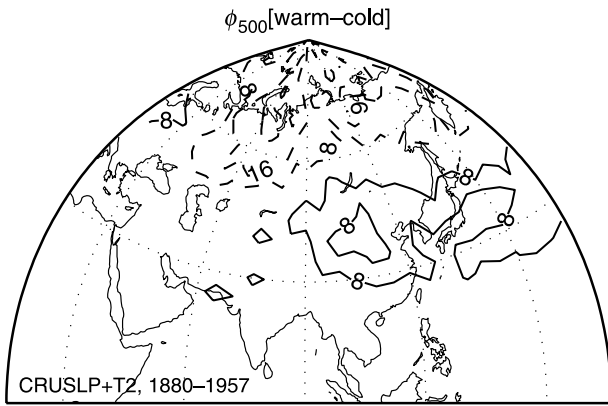


**Fig. 12.** Composite map of December–February 500 hPa heights using CRUSLP+T2 reconstruction with respect to the winter temperature extremes in East China. Warmest three winters (1934/35, 1945/46, 1948/49) minus coldest five years (1884/85, 1892/93, 1935/36, 1944/45, 1956/57). Unit: m

1 mainly covering about 60–70° N, 60–80° E with a  
 2 centre located over the Ural Mountains, and posi-  
 3 tive signals in the mid-latitudes of East Asia,  
 4 chiefly located over 40–45° N, 100–120° E. This  
 5 circulation pattern indicates that the enhanced  
 6 ridge over the Ural Mountains and deepened  
 7 trough over East Asia plays an important role in  
 8 the occurrence of extremely cold winters in East  
 9 China. This situation provides favourable condi-  
 10 tions for cold air masses to extend southward  
 11 over East Asia under the steering of upper cir-  
 12 culation along the enhanced airstream in the east  
 13 flank of the ridge and the rear of the trough  
 14 (Zhang and Lin, 1992; Gong et al., 2001).

### 15 5.2 ENSO-related circulation over Pacific/ 16 North America sector

17 The second application focusses on ENSO-related  
 18 changes in 500 hPa height in the Pacific–North  
 19 America sector. ENSO is one of the major sig-  
 20 nals for monitoring and predicting extra tropical  
 21 atmospheric circulation and climates. Brief re-  
 22 sults are presented which show that the time-lag  
 23 ENSO signals are well documented in reconstruct-  
 24 ed extra tropic 500 hPa heights.

25 Figure 13 displays the time-lag correlation be-  
 26 tween June and August Niño3 SST (Kaplan et al.,  
 27 1998) and December–February 500 hPa height  
 28 anomalies. Notice that the results shown here  
 29 are for the SST leading 500 hPa height by half  
 30 year. Centres of negative anomalies are evidently

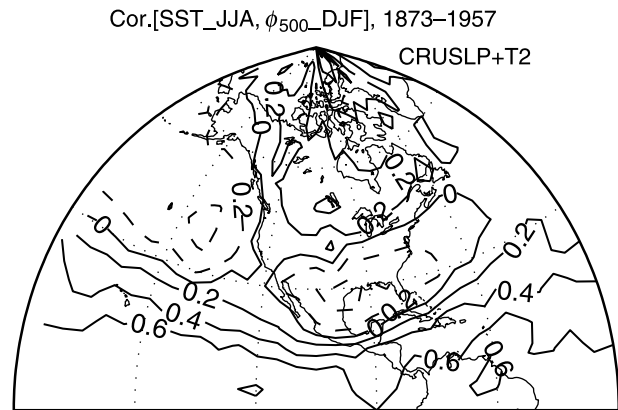


**Fig. 13.** Correlation of June–August Niño3 SST with December–February 500 hPa height of CRUSLP+T2 reconstruction. Data period is 1873–1957. SST leads height by 6 months

located in the northwestern North Pacific and 31  
 the southeastern U.S., while positive anomalies 32  
 appear in Canada as well as in a broad region 33  
 over the tropical Pacific. This well-defined struc- 34  
 ture clearly manifests the Pacific/North America 35  
 (PNA) teleconnection pattern. This feature is 36  
 even more significant in the simultaneous correla- 37  
 tion map. The PNA pattern is the dominant 38  
 mode of seasonal/interannual variability over the 39  
 Pacific/North America sector and plays a very 40  
 important role in Northern Hemisphere circulation 41  
 and climate predictability (e.g. Leathers et al., 42  
 1991; Renwick and Wallace, 1995, among many 43  
 others). Although PNA is an internal mode, its 44  
 variability is linked to tropical Pacific SST forc- 45  
 ing (Horel and Wallace, 1981). It is a fact that 46  
 in the reconstruction procedure, SSTs are used as 47  
 predictors, but only SSTs for months –1, 0, and 48  
 +1 are included in the predictor candidate matrix. 49  
 The strong persistence of the ENSO signals in- 50  
 volving the PNA pattern in the historical time 51  
 period in our reconstructions is impressive, even 52  
 for 500 hPa height lags behind Niño3 SST as long 53  
 as 6 months. Strong circulation links beyond 54  
 2-month time-lag should not be considered as a 55  
 simultaneous fitting to the SSTs, instead atmo- 56  
 spheric dynamics should play, at least partial, 57  
 roles. Therefore, our reconstruction provides an 58  
 opportunity to better understand how the north- 59  
 ern extra tropical climate has responded to ENSO 60  
 during the last one hundred years. 61

In general, the reconstructions might provide 62  
 useful information for general climate model 63

validation and the assessment of the global climate simulation of the last century, which is one of the essential issues in global climate study (Houghton et al., 2001).

## 6. Conclusion

This study has developed an objective method and calculated the monthly mean 500 hPa height anomalies for all Northern Hemisphere grid-points ( $5^\circ$  latitude  $\times$   $5^\circ$  longitude resolution) from surface temperature and three different SLP data sets. For each target month, predictors were determined from the candidates of target and two adjacent months. A stepwise program was used to derive the multiple regression equations. Averaging over all grid-points and all months, the number of predictors in the final regression equations was about 8.1. Then the 500 hPa heights prior to 1958 were reconstructed using these regression equations.

RE scores for CRUSLP + T2 and NCARSLP + T2 cases were higher than for HadSLP1 + T2 during the cross-validation period of 1958–1997. These two cases also display a more stable RE than the HadSLP1 case. Reconstructions based on CRUSLP and NCARSLP data sets were highly correlated with NCEP/NCAR reanalysis at 0.74. For the case of HadSLP1 the correlation is somewhat smaller, 0.65. Long-term reconstructions by Luterbacher et al. (2002) over Europe and eastern North Atlantic are also highly consistent with our results. On average the temporal correlations to our results vary from 0.66 to 0.72 during the period 1871/1873/1899–1957.

Our reconstructions provide the possibility for analyzing and understanding Northern Hemispheric climate variations in the middle troposphere since the late 19th century as two brief applications demonstrated, and may also be used for climate simulation validation.

However, it should be pointed out that the reconstructions are somewhat noisy (for example, Fig. 9). Possible reasons include that (1) the calibration period might be too short to derive a stable relationship, and (2) the regression method is heavily based on some highly sensitive local predictors. To overcome these shortcomings, future work is planned to perform an accompanying reconstruction using PCA-regression and

taking into account newly updated SLP and temperature data sets.

## Acknowledgments

Authors thank Drs. David Parker and Tara Ansell at the Hadley Centre, and Steven Worley of UCAR for their help in providing SLP data sets. Thanks are due to P. D. Jones of the University of East Anglia for providing temperature and CRU SLP data, and to Jürg Luterbacher of the Institute of Geography of University of Bern for providing 500 hPa reconstructions over the eastern North Atlantic-European region. The High-Performance Computing Centre at University of Bergen provided the computing resources for this study when the first author visited the Nansen Environmental and Remote Sensing Center. The authors thank the three reviewers for their constructive comments on an early version of the manuscript. Yongqi Gao was supported by the Chinese Academy of Sciences Hundred Talent Project.

## References

- Allan RJ, Ansell TJ (2006) A new globally complete monthly historical mean sea level pressure data set (HadSLP2): 1850–2004. *J Climate* (accepted)
- Basnett T, Parker D (1997) Development of the Global Mean Sea Level Pressure Data Set GMSLP2. Climate Research Technical Note, 79, Hadley Centre, Meteorological Office, Bracknell, U.K. 16 pp plus Appendices
- Bengtsson L, Hagemann S, Hodges KI (2004) Can climate trends be calculated from reanalysis data? *J Geophys Res* 109(D11111). doi: 10.1029/2004JD004536
- Brönnimann S (2003) A historical upper air data set for the 1939–1944 period. *Int J Climatol* 23: 769–791
- Brönnimann S, Luterbacher J (2004) Reconstructing northern hemisphere upper-level fields during World War II. *Climate Dynamics* 22: 499–510
- Brönnimann S, Luterbacher J, Staehelin J, Svendby TM, Hansen G, Svenøe T (2004) Extreme climate of the global troposphere and stratosphere in 1940–42 related to El Niño. *Nature* 431: 971–974
- Casty C, Handorf D, Sempf M (2005a) Combined winter climate regimes over the north Atlantic/European sector 1766–2000. *Geophys Res Lett* 32(L13801). doi: 10.1029/2005GL022431
- Casty C, Handorf D, Raible CC, González-Rouco JF, Weisheimer A, Xoplaki E, Luterbacher J, Dethloff K, Wanner H (2005b) Recurrent climate winter regimes in reconstructed and modeled 500 hPa geopotential height fields over the north Atlantic/European sector 1659–1990. *Climate Dynamics* 24: 809–822
- Casty C, Wanner H, Luterbacher J, Esper J, Böhm R (2005c) Temperature and precipitation variability in the European Alps since 1500. *Int J Climatol* 25(14): 1855–1880
- Compo GP, Whitaker JS, Sardeshmukh PD (2006) Feasibility of a 100-year reanalysis using only surface pressure data. *Bull Amer Meteor Soc* 87: 175–189

- 1 Cook ER, Briffa KR, Jones PD (1994) Spatial regression  
2 methods in dendroclimatology – A review and compar-  
3 ison of two techniques. *Int J Climatol* 14: 379–402
- 4 García-Herrera R, Können GP, Wheeler DA, Prieto MR,  
5 Jones PD, Koek FB (2005) CLIWOC: a climatological  
6 database for the world's oceans 1750–1854. *Climatic*  
7 *Change* 73: 1–12
- 8 Gong D-Y, Ho C-H (2002) Siberian High and climate change  
9 over middle to high latitude Asia. *Theor Appl Climatol*  
10 72: 1–9
- 11 Gong D-Y, Ho C-H (2004) Intra-seasonal variability of  
12 wintertime temperature over East Asia. *Int J Climatol*  
13 24(2): 131–144
- 14 Gong D-Y, Wang S-W (1999) Long-term variability of  
15 the Siberian High and the possible influence of global  
16 warming. *Acta Geographica Sinica* 54(2): 125–133  
17 (in Chinese)
- 18 Gong D-Y, Wang S-W (2000) Experiments on the recon-  
19 struction of historical monthly mean northern hemispheric  
20 500 hPa heights from surface data. *J Trop Meteor* 16(2):  
21 148–154 (in Chinese)
- 22 Gong D-Y, Wang S-W, Zhu J-H (2001) East Asian winter  
23 monsoon and Arctic Oscillation. *Geophys Res Lett* 28:  
24 2073–2076
- 25 Horel JD, Wallace JM (1981) Planetary scale atmospheric  
26 phenomena associated with the Southern Oscillation.  
27 *Mon Wea Rev* 109: 813–829
- 28 Houghton JT, Ding Y-H, Griggs DJ, Noguer M, van der  
29 Linden PJ, Dai X-S, Maskell K, Johnson CA (2001)  
30 *Climate Change 2001: the Scientific Basis. Contribution*  
31 *of Working Group I to the Third Assessment Report of the*  
32 *Intergovernmental Panel on Climate Change.* Cambridge,  
33 U.K.: Cambridge University Press, 881 pp
- 34 Jones PD (1987) The early twentieth century Arctic high –  
35 fact or fiction? *Climate Dynamics* 1: 63–75
- 36 Jones PD, Mann ME (2004) Climate over past millennia.  
37 *Rev Geophys* 42(RG2002). doi: 10.1029/2003RG000143
- 38 Jones PD, Moberg A (2003) Hemispheric and large-scale  
39 surface air temperature variations: an extensive revision  
40 and an update to 2001. *J Climate* 16: 206–223
- 41 Jones PD, New M, Parker DE, Martin S, Rigor IG (1999)  
42 Surface air temperature and its variations over the last 150  
43 years. *Rev Geophys* 37: 173–199
- 44 Jones PD, Osborn TJ, Briffa KR, Folland CK, Horton B,  
45 Alexander LV, Parker DE, Rayner NA (2001) Adjusting  
46 for sampling density in grid-box land and ocean surface  
47 temperature time series. *J Geophys* 106D: 3371–3380
- 48 Kalnay E, Kanamitsu M, Kistler R, Collins W, Deaven D,  
49 Gandin L, Iredell M, Saha S, White G, Woollen J, Zhu Y,  
50 Chelliah M, Ebisuzaki W, Higgins W, Janowiak J, Mo KC,  
51 Ropelewski C, Wang J, Leetmaa A, Reynolds R, Jenne R,  
52 Joseph D (1996) The NCEP/NCAR 40-year reanalysis  
53 project. *Bull Amer Meteor Soc* 77: 437–431
- 54 Kaplan A, Cane MA, Kushnir Y, Clement AC, Blumenthal  
55 MB, Rajagopalan B (1998) Analysis of global sea  
56 surface temperature 1856–1991. *J Geophys Res* 103:  
57 18567–18589
- 58 Kaplan A, Kushnir Y, Cane MA (2000) Reduced space op-  
59 timal interpolation of historical marine sea level pressure:  
60 1854–1992. *J Climate* 13(16): 2987–3002
- Klein WH, Dai Y (1998) Reconstruction of monthly mean  
700-mb heights from surface data by reverse specification.  
*J Climate* 11(8): 2136–2146
- Klein WH, Yang R (1986) Specification of monthly mean  
surface temperature anomalies in Europe and Asia from  
concurrent 700 mb monthly mean height anomalies over  
the Northern Hemisphere. *J Climatol* 6: 463–484
- Leathers DJ, Yarnal B, Palecki MA (1991) The Pacific/  
North American teleconnection pattern and United States  
climate. Part I: Regional temperature and precipitation  
associations. *J Climate* 4(5): 517–528
- Luterbacher J, Rickli R, Tinguely C, Xoplaki E, Schüpbach  
E, Dietrich D, Hüsler J, Ambühl M, Pfister C, Beeli P,  
Dietrich U, Dannecker A, Davies TD, Jones P, Slonosky  
V, Ogilvie AEJ, Maheras P, Kolyva-Machera F, Martin-  
Vide J, Barriendos M, Alcoforado MJ, Nunes MF, Jónsson  
T, Glaser R, Jacobeit J, Beck C, Philipp A, Beyer U, Kaas  
E, Schmith T, Barring L, Jönsson P, Rácz L, Wanner H  
(2000) Reconstruction of monthly mean sea level pres-  
sure over Europe for the late Maunder minimum period  
(1675–1715). *Int J Climatol* 20: 1049–1066
- Luterbacher J, Xoplaki E, Dietrich D, Rickli R, Jacobeit J,  
Beck C, Gyalistras D, Schmutz C, Wanner H (2002)  
Reconstruction of sea level pressure fields over the eastern  
north Atlantic and Europe back to 1500. *Climate Dynamics*  
18(7): 545–561
- Mann ME, Rutherford S, Wahl E, Ammann C (2005) Testing  
the fidelity of methods used in proxy-based reconstruc-  
tions of past climate. *J Climate* 18: 4097–4107
- Namias J (1944) Construction of 10000-foot pressure charts  
over ocean areas. *Bull Amer Meteor Soc* 25: 175–182
- Polansky B (2002) Reconstructing 500-hPa height fields  
over the northern hemisphere. Msc thesis, University of  
Washington
- Raible CC, Stocker TF, Yoshimori M, Renold M, Beyerle U,  
Casty C, Luterbacher J (2005) Northern hemispheric trends  
of pressure indices and atmospheric circulation patterns in  
observations, reconstructions, and coupled GCM simula-  
tions. *J Climate* 18: 3968–3982
- Rayner NA, Parker DE, Horton EB, Folland CK, Alexander  
LV, Rowell DP, Kaplan A, Kent EC (2003) Globally  
complete analyses of sea surface temperature, sea ice and  
night marine air temperature, 1871–2000. *J Geophys Res*  
108(D14):4407. doi: 10.1029/2002JD002670
- Renwick JA, Wallace JM (1995) Predictable anomaly patterns  
and the forecast skill of the northern hemisphere wintertime  
500-mb height field. *Mon Wea Rev* 123: 114–2131
- Rutherford S, Mann ME, Delworth TL, Stouffer RJ (2003)  
Climate field reconstruction under stationary and nonsta-  
tionary forcing. *J Climate* 16: 462–479
- Rutherford S, Mann ME, Osborn TJ, Bradley RS, Briffa KR,  
Hughes MK, Jones PD (2005) Proxy-based northern  
hemisphere surface temperature reconstructions: sensitiv-  
ity to methodology, predictor network, target season and  
target domain. *J Climate* 18: 2308–2329
- Schmutz C, Gyalistras D, Luterbacher J, Wanner H (2001)  
Reconstruction of monthly 700, 500 and 300 hPa geopo-  
tential height fields in the European and eastern north  
Atlantic region for the period 1901–1947. *Climate*  
*Research* 18(3): 181–193

- 1 Smith TM, Reynolds RW, Livezey RE, Stokes DC (1996) Xoplaki E, Luterbacher J, Paeth H, Dietrich D, Steiner N, 17  
2 Reconstruction of historical sea surface temperatures Grosjean M, Wanner H (2005) European spring and au- 18  
3 using empirical orthogonal functions. *J Climate* 9(6): tumn temperature variability and change of extremes over 19  
4 1403–1420 the last half millennium. *Geophys Res Lett* 32(L15713). 20  
5 Trenberth KE, Paolino DA (1980) The northern hemisphere doi: 10.1029/2005GL023424 21  
6 sea-level pressure data set: trends, errors and disconti- Zhang J-C, Lin Z-G (1992) *Climate of China*. John Wiley & 22  
7 nuities. *Mon Wea Rev* 104: 1354–1361 Sons and Shanghai Scientific and Technical Press, 376 pp 23  
8 Wang S-W, Gong D-Y, Chen Z-H (1999) Serious climatic 24  
9 disasters of China during the past 100 years. *Quart J Appl Meteor* 10(Suppl): 4353 (in Chinese) 25  
10 Wilks DS (1995) *Statistical methods in the atmospheric Authors' addresses: Dao-Yi Gong (e-mail: gdy@bnu. 26*  
11 sciences: an introduction. U.S.A.: Academic Press, edu.cn), Key Laboratory of Environmental Change and 27  
12 467 pp Natural Disaster, College of Resources Science and Technol- 28  
13 Wu B-Y, Wang J (2002) Winter Arctic Oscillation, Siberian ogy Beijing Normal University, Beijing 100875, China; 29  
14 High and East Asian winter monsoon. *Geophys Res Lett* Helge Drange, Bjerknes Center for Climate Research/  
15 29: 1897. doi: 10.1029/2002GL015373 Nansen Environmental and Remote Sensing Center, Univer- 30  
16 sity of Bergen, Norway; Yong-Qi Gao, Nansen-Zhu Interna- 31  
33 tional Research Center, IAP, Beijing 100029, China. 32